Fluorescent Probes Hot Paper

How to cite:
International Edition: doi.org/10.1002/anie.202016105
German Edition: doi.org/10.1002/ange.202016105

Fluorescent Membrane Tension Probes for Early Endosomes

Francesca Piazzolla[+], Vincent Mercier[+], Lea Assies, Naomi Sakai, Aurelien Roux, and Stefan Matile**

Abstract: *Fluorescent flipper probes have been introduced recently to image membrane tension in live cells, and strategies to target these probes to specific membranes are emerging. In this context, early endosome (EE) targeting without the use of protein engineering is especially appealing because it translates into a fascinating transport problem. Weakly basic probes, commonly used to track the inside of acidic late endosomes and lysosomes, are poorly retained in EE because they are sufficiently neutralized in weakly acidic EE, thus able to diffuse out. Here, we disclose a rational strategy to target EE using a substituted benzylamine with a higher pK_a value as a head group of the flipper probe. The resulting EE flippers are validated for preserved mechanosensitivity, ready for use in biology, particularly to elucidate the mechanics of endocytosis.*

The imaging of physical forces in biology with small-molecule fluorescent probes that can be added to unmodified living systems is a scientific challenge that calls for solutions from chemistry. The use of standard physics tools is mostly limited to the exterior and is quite perturbing to the system. Bioengineered tension sensors mostly use FRET pairs that report on structural changes of protein or DNA constructs in specific model systems and are not mechanosensitive by themselves.[1] These approaches do not satisfy the demand from mechanobiology for small-molecule fluorescent probes that are intrinsically mechanosensitive and work in unmodified cells at the location of interest. As a possible strategy to uncover such chemistry tools, we have introduced flipper probes.[2,3] They are constructed around dithienothiophene[4] dimers that are twisted out of co-planarity by repulsion between methyls and sulfurs next to the twistable bond (Figure 1e). Their planarization shifts absorption and excitation maxima to the red and increases fluorescence intensity and lifetime. The redshift originates from the mechanochemical increase of the ground-state energy and the lowering of the less twisted Franck-Condon (FC) excited-state energy.[5] The less twisted FC state preferentially relaxes to the emissive planar intramolecular charge transfer (PICT) state rather than to the more distorted non-emissive relaxation pathways to increase intensity and lifetime.[5] Contrary to most other small-molecule membrane probes[6,7] such as molecular rotors[6] that respond off-equilibrium in the excited state and report on viscosity, planarizable push-pull flipper probes thus respond at equilibrium in the ground state to physical forces from a confining environment.

In organic solvents, the planarizable push–pull probes absorb in the near-UV region, and do not fluoresce in water. The ordered environment of lipid bilayers increases their red shifts and the fluorescence lifetimes as expected from polarizing planarization. According to fluorescence lifetime imaging microscopy (FLIM), membrane tension applied with micropipettes or osmotic stress to mixed membranes, including biomembranes, increases lifetimes due to membrane reorganization with the dominant response from fully planarized flippers in highly-ordered microdomains composed of out-sorted un-stretchable lipids (Figure 1f),[3] together with decreasing membrane deformations.

For local membrane tension measurements in living cells, flipper probes must be placed in the membrane of interest (MOI). We already reported flipper localization strategies using either the more empirical chemistry known from trackers[8] or the general, rational design known from fusion proteins, e.g., HaloFlippers targeting HaloTags expressed in the MOI.[9] In this context, early endosomes (EE) attracted our attention. They are the first endosomal compartment reached by molecules endocytosed in vesicles (Figure 1d). At this sorting station, they can be recycled to the surface or sent toward late endosome (LE) and lysosome (LY), the latter depending on the endosomal sorting complex required for transport III (ESCRT-III). The importance of membrane tension in endolysosomal dynamics,[10,11] including the regulation of ESCRT-III, called for a precisely localized imaging of membrane tension in the EE. EE targeting is possible by engineering fusion proteins or labeling receptors at the cell surface and then following their endocytosis (vide infra),[11,12] but rarely by small-molecule probes. From EE to LE and LY, the acidity in the organelle increases (Figure 1d). This gradually decreasing pH has been much used for halochromic imaging,[13] endocytosis inhibition,[14] and endosomal escape[15,16] (proton sponge effect[16]). The pH gradients are also routinely used for targeting LE and LY[17] but not EE.[18] This question interested us because it translates EE targeting into a fascinating transport problem,[19–21] that is irreversible penetration by unidirectional translocation along a weak pH gradient. In the following, we tackle this subtle transport challenge and introduce EE flipper **1** (Figure 1e).

LysoTrackers function with an ammonium cation with a $pK_a \approx 7.4$, often morpholinium, also used in flipper **2** (Figure 1b).[17,8] In the cytosol, around pH 7,[22] these ammonium cations stay mostly protonated. However, since pK_a

[*] Dr. F. Piazzolla,[+] Dr. V. Mercier,[+] L. Assies, Dr. N. Sakai, Prof. A. Roux, Prof. S. Matile
School of Chemistry and Biochemistry, National Centre of Competence in Research (NCCR) Chemical Biology, University of Geneva, Geneva (Switzerland)
E-mail: aurelien.roux@unige.ch
stefan.matile@unige.ch
Homepage: https://www.unige.ch/sciences/chiorg/matile/
[+] These authors contributed equally to this work.
Supporting information and the ORCID identification number(s) for the author(s) of this article can be found under: https://doi.org/10.1002/anie.202016105.

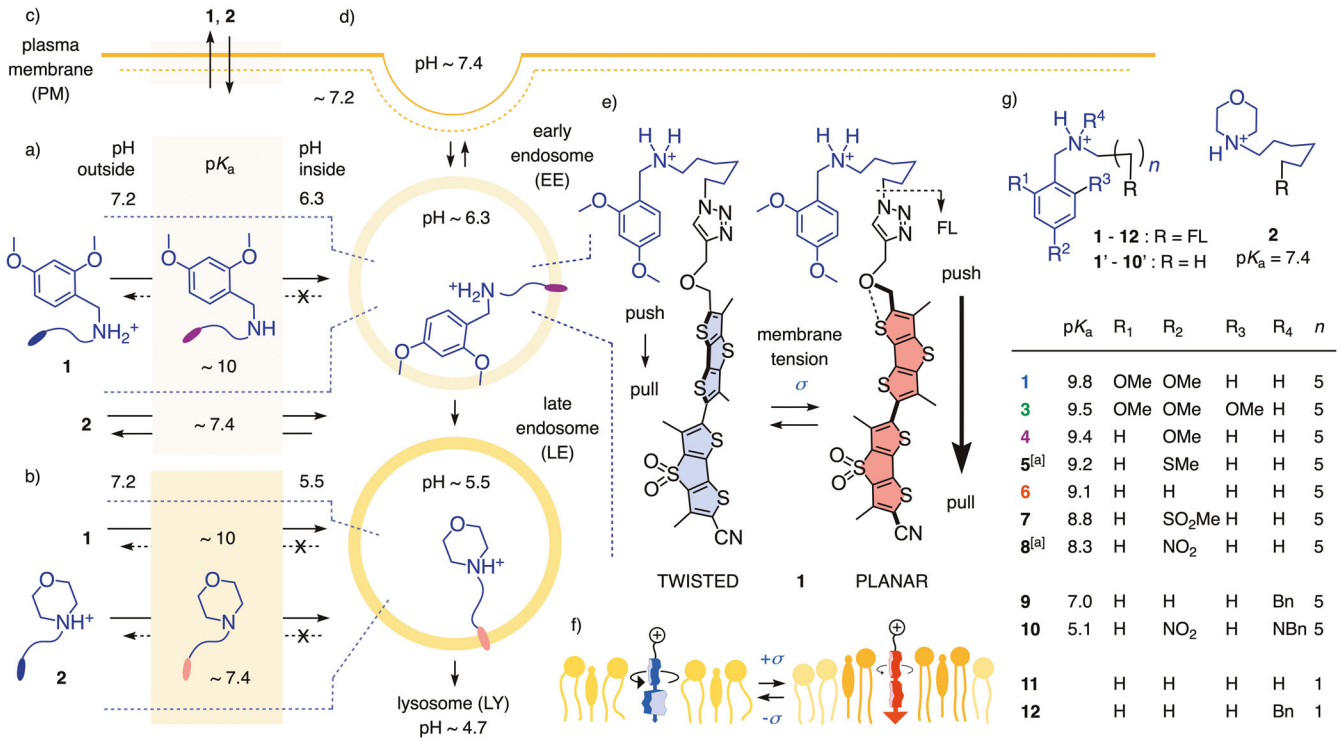

	pK_a	R_1	R_2	R_3	R_4	n
1	9.8	OMe	OMe	H	H	5
3	9.5	OMe	OMe	OMe	H	5
4	9.4	H	OMe	H	H	5
5[a]	9.2	H	SMe	H	H	5
6	9.1	H	H	H	H	5
7	8.8	H	SO_2Me	H	H	5
8[a]	8.3	H	NO_2	H	H	5
9	7.0	H	H	H	Bn	5
10	5.1	H	NO_2	H	NBn	5
11		H	H	H	H	1
12		H	H	H	Bn	1

Figure 1. Labeling of a) early endosomes with weakly acidic ammonium cations **1** by unidirectional penetration along a weak pH gradient, b) coinciding with conventional LE tracking along a stronger pH gradient and c) preceded by directionless plasma membrane (PM) penetration; compared to more acidic control **2** for LE tracking (b) together with directionless penetration of EE (a) and PM (c). d) The increase of acidity within organelles during endocytosis from PM to EE, LE, and LY. e,f) Structure and mode of action of EE flippers **1**. g) Structure of EE flipper **1** compared to LE flipper **2** and **3**–**12**, and flipper-free model head groups **1′-10′** with pK_a values from NMR titrations. FL = flipper, as in (e). See Figure S1 for full structures of flippers. The exchangeable counterions of cationic flippers, synthesized as TFA salts, are omitted. [a] Models **5′** and **8′** available, flippers **5** and **8** not (unstable). NBn = *p*-nitrobenzyl.

values depend significantly on the polarity of the environment,[23,19] the ammonium cation in **2** can temporarily release its proton to diffuse across the hydrophobic barrier as the neutral conjugate amine base of **2**, and re-protonate at the other side. Inside LE and LY at pH $\leq$ 5.5 with a $pK_a \approx 7.4$, this temporary deprotonation becomes impossible. As a result, the ammonium cation **2** is trapped, cannot move back to the cytosol. With time, this irreversible unidirectional penetration causes the cation **2** to accumulate in LE and LY, and thus label both. Similar mechanisms account for the loading of weakly basic drugs in liposomal delivery systems.[24] Temporary changes of pK_a by up to four orders of magnitude also allow carboxylates and fluoride to move across bilayer membrane as neutral conjugate acids.[19] Related proximity effects are ubiquitous in enzymes to produce amines and carboxylic acids in neutral water for base and acid catalysis, respectively, including aldolases, glycosidase, cholesterol cyclase, HIV protease, and so on.[25] However, in a biological context, pK_a changes beyond four orders of magnitude are rare.[26] The best example is the guanidinium cation with $pK_a \approx 12.5$, which accounts for the translocation of arginine-rich cell-penetrating peptides through repulsion-driven ion pairing rather than transient deprotonation.[21]

EE are poorly labeled by this method because the pH gradient is insufficient (Figure 1 a). The morpholino flipper **2** enters the EE by temporary deprotonation, just like LE and LY. However, the acidity within EE is insufficient to prevent deprotonation and inhibit the return into the cytosol, i.e., achieve the irreversible penetration needed for retention and labeling. These considerations suggested that what would be needed to target EE are less acidic ammonium cations. However, low acidity should also prevent deprotonation in the cytosol and thus inhibit translocation across any membrane.[21] The rare use of pK_a finetuning in EE trackers[18] suggested that the involved gradients are too weak, and the challenge cannot be met. In the following, we show that this impression is incorrect.

We selected benzyl substituted ammonium cations as head groups of potential EE flippers **1**, **3**–**12** (Figure 1 g). The acidity of these ammonium cations can be readily modulated by the attached electron-donating or withdrawing substituents on the phenyl rings. The number of nitrogen substituents and the tethers length were also expected to influence the pK_a. Further, phenyl groups are suited for a membrane probe since aromatic-lipid bilayer interactions are well known from membrane proteins to assist their translocation and anchoring at the interface,[27,28] presumably by cation-π interactions with the choline headgroup of many lipids.[27]

Flippers **1**, **3**, **4**, **6**, **7**, **9**–**12**, and controls **1′-10′** used in this study were prepared by multistep synthesis similar to that of LY-flipper **2** (Schemes S1–S4). Reductive amination reactions between the substituted benzaldehydes and amines provided

different mono- and di-benzyl amines easily. The obtained benzylamines with an azide terminus then underwent azide-alkyne click reactions with a common flipper intermediate with an alkyne terminus to give desired flippers. Among the EE-flipper candidates, *p*-thiomethyl- and *p*-nitro-benzyl flippers **5** and **8** were inaccessible due to their instability caused by photoinduced oxidation and debenzylation (Figure S28), respectively. The pK_a values of hydrophobic models **1′–10′** without the flipper mechanophore were estimated to range between 5.1 and 9.8 by pH titration using ^{1}H NMR spectroscopy (Figures 1 g, S2–S27).

EE labeling was evaluated by co-localization with the epidermal growth factor (EGF) labeled with Alexa-647 (Far-Red, FR) to avoid overlap with flipper fluorescence (Figures 2, S29–S33, S37b). In this standard pulse-chase endocytosis assay,[11,29] EGF-FR mainly labels EE after a 10 minute incubation of cells (pulse) and LE and LY when pulse is followed by a 2 hour incubation in a medium without EGF-FR (chase). During the last 10 minutes of the above process, cells were incubated with specific flipper probes because they rapidly label the compartments compatible with their pK_a. Complete labeling of LE and LY within ≈6 minutes as well as the absence of plasma membrane staining[8] confirmed that flippers enter cells and organelles by directional penetration as outlined in Figure 1 a–c, and not by endocytosis, which would take ≈2 hours for LE and LY, rather than 6 minutes (Figure 1 d, 2).

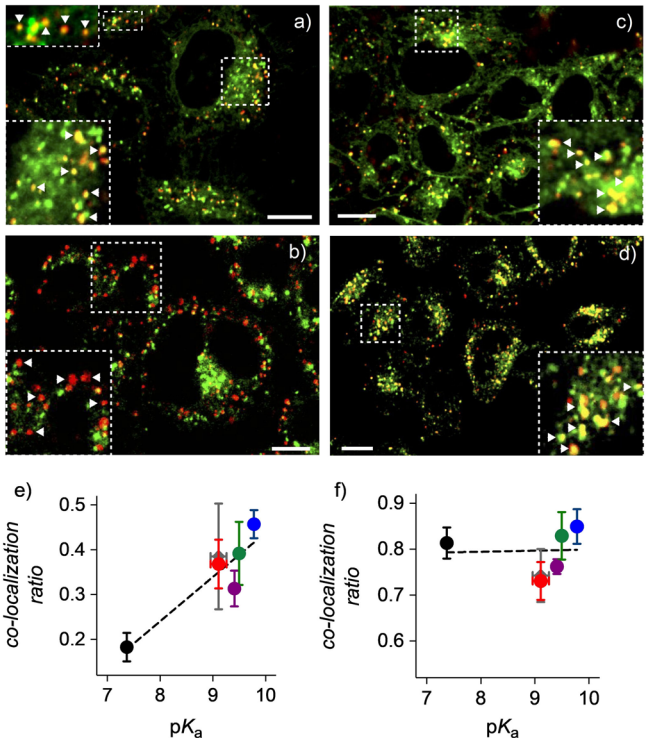

Figure 2. a–d) Merged CLSM images of HeLa MZ cells labeled with **1** (a,c), or **2** (b,d, 1 μM, green) and EGF-FR (red) after 10 min pulse (a,b) or 10 min pulse followed by 2 h chase (c,d). Insets: zoomed portions of images with arrows pointing at the EGF-FR labeled endosomes (note how with their small size, yellow dots can appear red without magnification; (a), top left, compare (e,f)). Scale bars = 10 μm. e) Fractions of EGF-FR labeled organelles co-localized with **1** (blue ●), **2** (black ●), **3** (green ●), **4** (violet ●), **6** (red ●), or **11** (grey ◆, 1 μM) after 10 min chase (mean ± SD). f) As (e), after 2 h chase.

Confocal laser scanning microscopy (CLSM) images of HeLa MZ cells labeled with EGF-FR (red) and flipper **1** (green) for 10 minutes were taken (Figure 2 a). Since flipper **1** also labels LE and LY, the global co-localization with EGF-FR cannot be high (green vs. yellow). However, the proportion of EGF-FR co-localized with flipper **1** was significant (red vs. yellow). This result contrasted with LY-flipper **2**, which was practically excluded from EGF-FR labeled EE (Figure 2 b). After a 2 hour chase, EGF-FR in LE co-localized equally well with both flippers (Figure 2 c,d).

Co-localization of EGF-FR and various flippers was quantified using automated high-content microscopy (Figure 2 e,f).[30] This method allowed us to analyze thousands of cells in a short time. Dibenzylamino-flippers **9**, **10**, and **12** were excluded from the analysis because of their poor staining. Also abandoned was the SO_2Me substituted flipper **7** because it was unstable in the media due to debenzylation (Figure S28). For the remaining six flippers, co-localization ratios were determined from the ratio of co-labeled organelles and all organelles labeled with EGF-FR (Figure 2 e,f). The results obtained after 10 minutes of pulse showed a clear correlation between co-localization ratios and the pK_a of the ammonium cations, as expected for EE labeling (Figure 2 e). After a 2 hour chase, this correlation vanished, and co-localization ratios were high and constant, independent of the pK_a of the ammonium cations as expected for LE/LY labeling (Figure 2 f). A comparison of benzylamine flippers with a long (Figure 2 e, **6** red ●) or short tether (**11** grey ◆) revealed poor reproducibility with the latter and thus confirmed that the former, as in the original morpholino flipper **2**, is preferable for acidity screening.

Overall less than perfect co-localization is intrinsic to EGF-FR labeling, which produces a broader distribution along the endocytic pathway with, for instance, a few LE already labeled when most EGF-FR is still in the EE and a few EE remaining labeled when most EGF-FR has reached the LE (Figure 2). The use of classical LysoTrackers instead was not meaningful because EEs remain invisible. According to the mean fluorescence intensities, the efficiency of probe internalization in cells did not correlate with the pK_a of the ammonium cations (Figure S34). We also have not observed PM staining with this series of flippers. Thus, these results indicated that the higher limit of pK_a to prevent the deprotonation in the membrane is still not reached with flipper **1**.

The mechanosensitivity of EE flipper **1** was explored with FLIM. Very weak and diffuse background fluorescence with flipper **1**, at least one order of magnitude less intense than the tiny endosomes, was removed by adjusting the threshold of the number of photons per pixel. Average lifetimes (τ_1) of all labeled organelles by flipper **1**, including EE, LE, and LY, were around $\tau = 4.42$ ns. This was significantly lower than for LY flipper **2** ($\tau = 4.60$ ns), suggesting that probe **1** is in a more liquid-disordered membrane, as expected from its EE localization (Figure 3 a,c, blue, S37a).[8,11] The application of hyperosmotic stress lowered the lifetime to $\tau = 4.21$ ns (Fig-

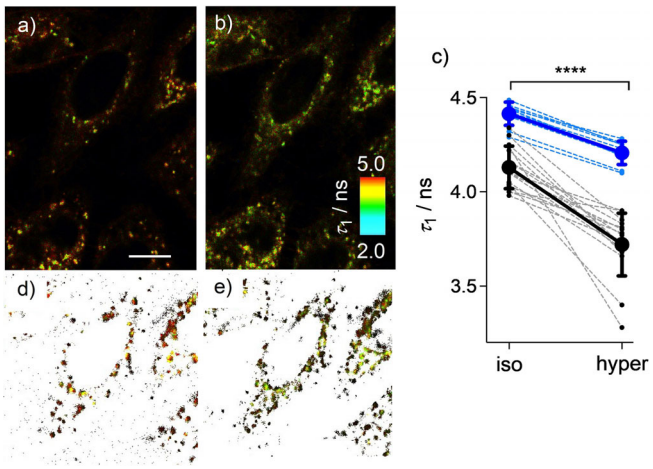

Figure 3. a,b,d,e) FLIM images of **1** (1 μM) in HeLa MZ cells before (a,d) and after hypertonic shock (b,e) without (a,b) and with EE filtering using the 10-min internalized A647-Dextran image (d,e). Scale bar = 10 μm. c) Fluorescent lifetimes under isotonic (iso) and hypertonic (hyper) conditions, all pixels (blue) or only pixels corresponding to EE (black). Symbols with error bars represent the mean values ± SD, dashed lines the individual fields from 3 independent experiments. Two-tailed paired Student's *t*-tests gave $P < 0.0001$ (****) for the two set of data.

ure 3b,c, blue). Originating from the tension-induced disassembly of ordered microdomains or increasing membrane deformations, this decrease was consistent with flipper deplanarization in response to decreasing membrane tension under hyperosmotic conditions.[3,8,9] It thus validated EE flipper **1** as an operational membrane tension probe.

EE specific membrane tension changes were extracted by applying a filter based on the co-localization with A647-dextran (Figures 3d,e,c, black). A647-dextran was selected because this probe, like EGF-FR, is not excited by the 485 nm pulsed laser used for FLIM, emission (670 nm) is outside the 550–650 nm range used to collect photons, and the distance from flippers in the membrane to A647-dextran in the lumen is much too long for FRET. Controls confirmed that A647-dextran does not significantly affect the overall lifetime histogram of EE flipper **1** (Figure S37b). The average lower lifetime of EE specific pixels ($\tau = 4.13$ ns vs. 4.42 ns for all endosomes) and the larger lifetime change upon application of the hyperosmotic stress ($\Delta\tau = 0.4$ ns vs. 0.2 ns) were further supporting that flippers are sensitive to the different properties of less ordered EE and more ordered LE/LY membranes and their response to tension (Figure 3c).[31]

Overall, the obtained results demonstrate that protein-free EE membrane labeling can be conceived as an intriguing transport challenge[19–21] that can be addressed by rational design (Figure 1). Namely, the labeling of LE but not EE by flipper **2** is dictated by the high acidity of the ammonium cation with a $pK_a \approx 7.4$, allowing the translocation across the membrane at pH ≈ 7.2 and retention at pH ≈ 5.5 but not at pH ≈ 6.3 (Figure 1a–c). In flipper **1**, the acidity is with $pK_a = 9.8$ sufficiently lowered to assure its retention at pH ≈ 6.3 to label the EE (Figure 1a). Fascinated by the subtle precision required for operational EE targeting by unidirectional penetration, we currently aim to map out the full pK_a range and identify the maximum. Meanwhile, the here introduced EE flipper **1** is ready for use in biology, without the need for cellular engineering or possible interference from proteins used for targeting. The simple addition of the fluorescent probe to unmodified cells is particularly attractive to study the mechanics of endocytosis.[10,11]

Acknowledgements

We thank D. Moreau and S. Vossio (University of Geneva) for help with high-content microscopy and analysis, the NMR, the MS, and the Bioimaging and ACCESS platforms for services, and the University of Geneva, the Swiss National Centre of Competence in Research (NCCR) Molecular Systems Engineering, the NCCR Chemical Biology, and the Swiss NSF for financial support.

Conflict of interest

The University of Geneva has licensed four Flipper-TR® probes to Spirochrome for commercialization, including **2**, but not **1**.

Keywords: directionality · early endosomes · fluorescent probes · mechanosensitivity · membrane penetration · pH gradients

[1] a) Y. Liu, K. Galior, V. P.-Y. Ma, K. Salaita, *Acc. Chem. Res.* **2017**, *50*, 2915–2924; b) C. Grashoff, B. D. Hoffman, M. D. Brenner, R. Zhou, M. Parsons, M. T. Yang, M. A. McLean, S. G. Sligar, C. S. Chen, T. Ha, M. A. Schwartz, *Nature* **2010**, *466*, 263–266; c) E. J. Aird, K. J. Tompkins, M. P. Ramirez, W. R. Gordon, *ACS Sens.* **2020**, *5*, 34–39; d) G. A. Shamsan, D. J. Odde, *Curr. Opin. Chem. Biol.* **2019**, *53*, 125–130; e) R. Jöhr, M. S. Bauer, L. C. Schendel, C. Kluger, H. E. Gaub, *Nano Lett.* **2019**, *19*, 3176–3181; f) E. M. Gates, A. S. LaCroix, K. E. Rothenberg, B. D. Hoffman, *Cytometry Part A* **2019**, *95*, 201–213.

[2] a) A. Fin, A. Vargas Jentzsch, N. Sakai, S. Matile, *Angew. Chem. Int. Ed.* **2012**, *51*, 12736–12739; *Angew. Chem.* **2012**, *124*, 12908–12911; b) M. Dal Molin, Q. Verolet, A. Colom, R. Letrun, E. Derivery, M. Gonzalez-Gaitan, E. Vauthey, A. Roux, N. Sakai, S. Matile, *J. Am. Chem. Soc.* **2015**, *137*, 568–571.

[3] A. Colom, E. Derivery, S. Soleimanpour, C. Tomba, M. D. Molin, N. Sakai, M. González-Gaitán, S. Matile, A. Roux, *Nat. Chem.* **2018**, *10*, 1118–1125.

[4] K. Strakova, L. Assies, A. Goujon, F. Piazzolla, H. V. Humeniuk, S. Matile, *Chem. Rev.* **2019**, *119*, 10977–11005.

[5] T. Kato, K. Strakova, J. García-Calvo, N. Sakai, S. Matile, *Bull. Chem. Soc. Jpn.* **2020**, *93*, 1401–1411.

[6] a) J. A. Robson, M. Kubánková, T. Bond, R. A. Hendley, A. J. P. White, M. K. Kuimova, J. D. E. T. Wilton-Ely, *Angew. Chem. Int. Ed.* **2020**, *59*, 21431–21435; *Angew. Chem.* **2020**, *132*, 21615–21619; b) M. Páez-Pérez, I. López-Duarte, A. Vyšniauskas, N. J. Brooks, M. K. Kuimova, *Chem. Sci.* **2021**, *12*, 2604–2613; c) C.-H. Wu, Y. Chen, K. A. Pyrshev, Y.-T. Chen, Z. Zhang, K.-H. Chang, S. O. Yesylevskyy, A. P. Demchenko, P.-T. Chou, *ACS Chem. Biol.* **2020**, *15*, 1862–1873; d) L. Yu, J. F. Zhang, M. Li, D. Jiang, Y. Zhou, P. Verwilst, J. S. Kim, *Chem. Commun.* **2020**, *56*, 6684–6687; e) K. Tan, Y. Chen, K. Ma, Q. Wang, X. Liu, F. Wang, *Small* **2019**, *15*, 1903266; f) I. E. Steinmark, A. L. James,

P.-H. Chung, P. E. Morton, M. Parsons, C. A. Dreiss, C. D. Lorenz, G. Yahioglu, K. Suhling, *PLoS One* **2019**, *14*, e0211165; g) W. Nakanishi, S. Saito, N. Sakamoto, A. Kashiwagi, S. Yamaguchi, H. Sakai, K. Ariga, *Chem. Asian J.* **2019**, *14*, 2869 – 2876; h) A. Jiménez-Sánchez, E. K. Lei, S. O. Kelley, *Angew. Chem. Int. Ed.* **2018**, *57*, 8891 – 8895; *Angew. Chem.* **2018**, *130*, 9029 – 9033; i) R. Guo, J. Yin, Y. Ma, Q. Wang, W. Lin, *J. Mater. Chem. B* **2018**, *6*, 2894 – 2900; j) J. E. Chambers, M. Kubánková, R. G. Huber, I. López-Duarte, E. Avezov, P. J. Bond, S. J. Marciniak, M. K. Kuimova, *ACS Nano* **2018**, *12*, 4398 – 4407; k) S. Akbulatov, Y. Tian, Z. Huang, T. J. Kucharski, Q. Z. Yang, R. Boulatov, *Science* **2017**, *357*, 299 – 303; l) M. A. Haidekker, E. A. Theodorakis, *J. Mater. Chem. C* **2016**, *4*, 2707 – 2718.

[7] a) A. S. Klymchenko, *Acc. Chem. Res.* **2017**, *50*, 366 – 375; b) D. I. Danylchuk, P.-H. Jouard, A. S. Klymchenko, *J. Am. Chem. Soc.* **2021**, *143*, 912 – 924; c) P. Liu, E. W. Miller, *Acc. Chem. Res.* **2020**, *53*, 11 – 19; d) M. Sundukova, E. Prifti, A. Bucci, K. Kirillova, J. Serrao, L. Reymond, M. Umebayashi, R. Hovius, H. Riezman, K. Johnsson, P. A. Heppenstall, *Angew. Chem. Int. Ed.* **2019**, *58*, 2341 – 2344; *Angew. Chem.* **2019**, *131*, 2363 – 2366; e) D. I. Danylchuk, S. Moon, K. Xu, A. S. Klymchenko, *Angew. Chem. Int. Ed.* **2019**, *58*, 14920 – 14924; *Angew. Chem.* **2019**, *131*, 15062 – 15066; f) Y. Xiong, A. Vargas Jentzsch, J. W. M. Osterrieth, E. Sezgin, I. V. Sazanovich, K. Reglinski, S. Galiani, A. W. Parker, C. Eggeling, H. L. Anderson, *Chem. Sci.* **2018**, *9*, 3029 – 3040; g) J. Daniel, C. Mastrodonato, A. Sourdon, G. Clermont, J.-M. Vabre, B. Goudeau, H. Voldoire, S. Arbault, O. Mongin, M. Blanchard-Desce, *Chem. Commun.* **2015**, *51*, 15245 – 15248.

[8] A. Goujon, A. Colom, K. Straková, V. Mercier, D. Mahecic, S. Manley, N. Sakai, A. Roux, S. Matile, *J. Am. Chem. Soc.* **2019**, *141*, 3380 – 3384.

[9] K. Straková, J. López-Andarias, N. Jiménez-Rojo, J. E. Chambers, S. J. Marciniak, H. Riezman, N. Sakai, S. Matile, *ACS Cent. Sci.* **2020**, *6*, 1376 – 1385.

[10] a) M. Riggi, C. Bourgoint, M. Macchione, S. Matile, R. Loewith, A. Roux, *J. Cell. Biol.* **2019**, *218*, 2265 – 2276; b) S. Boulant, C. Kural, J.-C. Zeeh, F. Ubelmann, T. Kirchhausen, *Nat. Cell Biol.* **2011**, *13*, 1124 – 1131.

[11] V. Mercier, J. Larios, G. Molinard, A. Goujon, S. Matile, J. Gruenberg, A. Roux, *Nat. Cell Biol.* **2020**, *22*, 947 – 959.

[12] a) E. C. Greenwald, S. Mehta, J. Zhang, *Chem. Rev.* **2018**, *118*, 11707 – 11794; b) Y. Han, X. Li, H. Chen, X. Hu, Y. Luo, T. Wang, Z. Wang, Q. Li, C. Fan, J. Shi, L. Wang, Y. Zhao, C. Wu, N. Chen, *ACS Appl. Mater. Interfaces* **2017**, *9*, 21200 – 21208; c) T. Albrecht, Y. Zhao, T. H. Nguyen, R. E. Campbell, J. D. Johnson, *Cell Calcium* **2015**, *57*, 263 – 274; d) M. Kerr, R. D. Teasdale, *Semin. Cell Dev. Biol.* **2014**, *31*, 11 – 19; e) Y. Zhang, M. Hensel, *Nanoscale* **2013**, *5*, 9296 – 9309; f) Z. Darwich, A. S. Klymchenko, D. Dujardin, Y. Mély, *RSC Adv.* **2014**, *4*, 8481 – 8488.

[13] a) M. Tian, C. Liu, B. Dong, Y. Zuo, W. Lin, *Chem. Commun.* **2019**, *55*, 10440 – 10443; b) S. Takahashi, Y. Kagami, K. Hanaoka, T. Terai, T. Komatsu, T. Ueno, M. Uchiyama, I. Koyama-Honda, N. Mizushima, T. Taguchi, H. Arai, T. Nagano, Y. Urano, *J. Am. Chem. Soc.* **2018**, *140*, 5925 – 5933; c) A. Wallabregue, D. Moreau, P. Sherin, P. Moneva Lorente, Z. Jarolímová, E. Bakker, E. Vauthey, J. Gruenberg, J. Lacour, *J. Am. Chem. Soc.* **2016**, *138*, 1752 – 1755; d) H. J. Kim, C. H. Heo, H. M. Kim, *J. Am. Chem. Soc.* **2013**, *135*, 17969 – 17977; e) S. Chen, Y. Hong, Y. Liu, J. Liu, C. W. T. Leung, M. Li, R. T. K. Kwok, E. Zhao, J. W. Y. Lam, Y. Yu, B. Z. Tang, *J. Am. Chem. Soc.* **2013**, *135*, 4926 – 4929; f) T. Myochin, K. Kiyose, K. Hanaoka, H. Kojima, T. Terai, T. Nagano, *J. Am. Chem. Soc.* **2011**, *133*, 3401 – 3409; g) N. Narayanaswamy, K. Chakraborty, A. Saminathan, E. Zeichner, K. Leung, J. Devany, Y. Krishnan, *Nat. Methods* **2019**, *16*, 95 – 102; h) A. Méndez Ardoy, J. J. Reina, J. Montenegro, *Chem. Eur. J.* **2020**, *26*, 7516 – 7536.

[14] a) C. Tietze, P. Schlesinger, P. Stahl, *Biochem. Biophys. Res. Commun.* **1980**, *93*, 1 – 8; b) E. Blanchard, S. Belouzard, L. Goueslain, T. Wakita, J. Dubuisson, C. Wychowski, Y. Rouillé, *J. Virol.* **2006**, *80*, 6964 – 6972.

[15] a) A. Kashiwada, M. Tsuboi, K. Matsuda, *Langmuir* **2011**, *27*, 1403 – 1408; b) V. Biju, T. Itoh, M. Ishikawa, *Chem. Soc. Rev.* **2010**, *39*, 3031 – 3056; c) Q. Sun, S. Cai, B. R. Peterson, *J. Am. Chem. Soc.* **2008**, *130*, 10064 – 10065.

[16] a) J.-P. Behr, *Chimia* **1997**, *51*, 34 – 36; b) J. V. V. Arafiles, H. Hirose, M. Akishiba, S. Tsuji, M. Imanishi, S. Futaki, *Bioconjugate Chem.* **2020**, *31*, 547 – 553.

[17] a) C. Benitez-Martin, J. A. Guadix, J. R. Pearson, F. Najera, J. M. Perez-Pomares, E. Perez-Inestrosa, *ACS Sens.* **2020**, *5*, 1068 – 1074; b) X. Zhao, C. Wang, G. Yuan, H. Ding, L. Zhou, X. Liu, Q. Lin, *Sens. Actuators B* **2019**, *290*, 79 – 86; c) S. Xia, M. Fang, J. Wang, J. Bi, W. Mazi, Y. Zhang, R. L. Luck, H. Liu, *Sens. Actuators B* **2019**, *294*, 1 – 13; d) C. Li, Y. Wang, S. Huang, X. Zhang, X. Kang, Y. Sun, Z. Hu, L. Han, L. Du, Y. Liu, *Talanta* **2018**, *188*, 316 – 324; e) X. Liu, Y. Su, H. Tian, L. Yang, H. Zhang, X. Song, J. W. Foley, *Anal. Chem.* **2017**, *89*, 7038 – 7045; f) M. Li, H. Ge, V. Mirabello, R. L. Arrowsmith, G. Kociok-Köhn, S. W. Botchway, W. Zhu, S. I. Pascu, T. D. James, *Chem. Commun.* **2017**, *53*, 11161 – 11164; g) M. Duvvuri, S. Konkar, R. S. Funk, J. M. Krise, J. P. Krise, *Biochemistry* **2005**, *44*, 15743 – 15749.

[18] a) F. Miao, S. Uchinomiya, Y. Ni, Y.-T. Chang, J. Wu, *ChemPlusChem* **2016**, *81*, 1209 – 1215; b) K. Zhou, H. Liu, S. Zhang, X. Huang, Y. Wang, G. Huang, B. D. Sumer, J. Gao, *J. Am. Chem. Soc.* **2012**, *134*, 7803 – 7811; c) K. Zhou, Y. Wang, X. Huang, K. Luby-Phelps, B. D. Sumer, J. Gao, *Angew. Chem. Int. Ed.* **2011**, *50*, 6109 – 6114; *Angew. Chem.* **2011**, *123*, 6233 – 6238.

[19] a) V. Gorteau, G. Bollot, J. Mareda, S. Matile, *Org. Biomol. Chem.* **2007**, *5*, 3000 – 3012; b) X. Wu, E. N. W. Howe, P. A. Gale, *Acc. Chem. Res.* **2018**, *51*, 1870 – 1879.

[20] a) G. Su, M. Zhang, W. Si, Z.-T. Li, J.-L. Hou, *Angew. Chem. Int. Ed.* **2016**, *55*, 14678 – 14682; *Angew. Chem.* **2016**, *128*, 14898 – 14902; b) A. D. Peters, S. Borsley, F. della Sala, D. F. Cairns-Gibson, M. Leonidou, J. Clayden, G. F. S. Whitehead, I. J. Vitórica-Yrezábal, E. Takano, J. Burthem, S. L. Cockroft, S. J. Webb, *Chem. Sci.* **2020**, *11*, 7023 – 7030; c) T. Muraoka, K. Umetsu, K. V. Tabata, T. Hamada, H. Noji, T. Yamashita, K. Kinbara, *J. Am. Chem. Soc.* **2017**, *139*, 18016 – 18023; d) H. Li, H. Valkenier, A. G. Thorne, C. M. Dias, J. A. Cooper, M. Kieffer, N. Busschaert, P. A. Gale, D. N. Sheppard, A. P. Davis, *Chem. Sci.* **2019**, *10*, 9663 – 9672.

[21] a) N. Chuard, K. Fujisawa, P. Morelli, J. Saarbach, N. Winssinger, P. Metrangolo, G. Resnati, N. Sakai, S. Matile, *J. Am. Chem. Soc.* **2016**, *138*, 11264 – 11271; b) H. Fernández-Caro, I. Lostalé-Seijo, M. Martínez-Calvo, J. Mosquera, J. L. Mascareñas, J. Montenegro, *Chem. Sci.* **2019**, *10*, 8930 – 8938; c) A. Walrant, A. Bauzá, C. Girardet, I. D. Alves, S. Lecomte, F. Illien, S. Cardon, N. Chaianantakul, M. Pallerla, F. Burlina, A. Frontera, S. Sagan, *Biochim. Biophys. Acta* **2020**, *1862*, 183098.

[22] J. R. Casey, S. Grinstein, J. Orlowski, *Nat. Rev. Mol. Cell Biol.* **2010**, *11*, 50 – 61.

[23] S. Tshepelevitsh, A. Kütt, M. Lõkov, I. Kaljurand, J. Saame, A. Heering, P. G. Plieger, R. Vianello, I. Leito, *Eur. J. Org. Chem.* **2019**, 6735 – 6748.

[24] T. D. Madden, P. R. Harrigan, L. C. L. Tai, M. B. Bally, L. D. Mayer, T. E. Redelmeier, H. C. Loughrey, C. P. S. Tilcock, L. W. Reinish, P. R. Cullis, *Chem. Phys. Lipids* **1990**, *53*, 37 – 46.

[25] a) T. D. Machajewski, C.-H. Wong, *Angew. Chem. Int. Ed.* **2000**, *39*, 1352 – 1375; *Angew. Chem.* **2000**, *112*, 1406 – 1430; b) V. L. Schramm, *ACS Chem. Biol.* **2013**, *8*, 71 – 81; c) K. U. Wendt, G. E. Schulz, E. J. Corey, D. R. Liu, *Angew. Chem. Int. Ed.* **2000**, *39*, 2812 – 2833; *Angew. Chem.* **2000**, *112*, 2930 – 2952.

[26] K. Fujisawa, M. Humbert-Droz, R. Letrun, E. Vauthey, T. A. Wesolowski, N. Sakai, S. Matile, *J. Am. Chem. Soc.* **2015**, *137*, 11047 – 11056.
[27] a) A. J. de Jesus, T. W. Allen, *Biochim. Biophys. Acta Biomembr.* **2013**, *1828*, 864 – 876; b) T. Broemstrup, N. Reuter, *Phys. Chem. Chem. Phys.* **2010**, *12*, 7487 – 7496; c) J. M. Sanderson, E. J. Whelan, *Phys. Chem. Chem. Phys.* **2004**, *6*, 1012 – 1017.
[28] a) H. Hong, S. Park, R. H. Flores Jiménez, D. Rinehart, L. K. Tamm, *J. Am. Chem. Soc.* **2007**, *129*, 8320 – 8327; b) W.-M. Yau, W. C. Wimley, K. Gawrisch, S. H. White, *Biochemistry* **1998**, *37*, 14713 – 14718; c) J. A. Killian, G. von Heijne, *Trends Biochem. Sci.* **2000**, *25*, 429 – 434.
[29] a) G. Carpenter, S. Cohen, *J. Cell Biol.* **1976**, *71*, 159 – 171; b) W. A. Dunn, T. P. Connolly, A. L. Hubbard, *J. Cell Biol.* **1986**, *102*, 24 – 36.
[30] D. Moreau, J. Gruenberg, *Chimia* **2016**, *70*, 878 – 882.
[31] G. van Meer, D. R. Voelker, G. W. Feigenson, *Nat. Rev. Mol. Cell Biol.* **2008**, *9*, 112 – 124.

Manuscript received: December 3, 2020
Revised manuscript received: January 18, 2020
Accepted manuscript online: February 3, 2021
Version of record online: ■■ ■■, ■■■■

Communications

Fluorescent Probes

F. Piazzolla, V. Mercier, L. Assies, N. Sakai, A. Roux,* S. Matile* _____ ■■■■–■■■■

Fluorescent Membrane Tension Probes for Early Endosomes

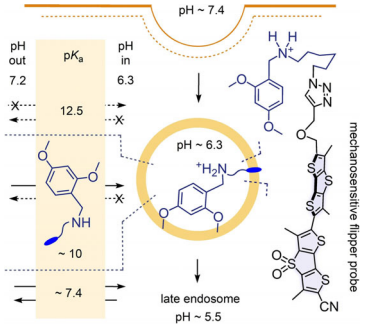

Unidirectional penetration along minimalist pH gradients is developed as a strategy to label the membrane of early endosomes with mechanosensitive flipper probes, by simple addition to unmodified cells. Substituted benzylamines offer the right acidity, pK_a = 10, not too strong to allow reversibility, not too weak to inhibit penetration from neutral water in the cytosol, and, perhaps, extra returns from interfacial aromatic anchoring.